Effects of an Intercalation Nanocomposite at the Photoanode/Electrolyte Interface in Quasi-Solid Dye-Sensitized Solar Cells

ARTICLE *in* THE JOURNAL OF PHYSICAL CHEMISTRY C · AUGUST 2011

Impact Factor: 4.77 · DOI: 10.1021/jp204466h

THE JOURNAL OF PHYSICAL CHEMISTRY C

ARTICLE

pubs.acs.org/JPCC

Effects of an Intercalation Nanocomposite at the Photoanode/Electrolyte Interface in Quasi-Solid Dye-Sensitized Solar Cells

Rui Gao, Liduo Wang,* Yi Geng, Beibei Ma, Yifeng Zhu, Haopeng Dong, and Yong Qiu

Key Lab of Organic Optoelectronics and Molecular Engineering of the Ministry of Education, Department of Chemistry, Tsinghua University, Beijing 100084, China

ABSTRACT: In this paper, interface effects of *N*-methyl-benzimidazole (NMBI) and a novel intercalation composite of NMBI and montmorillonite (MMT) were studied. The intercalation composite showed better interface modification effects than NMBI individually. The FTIR spectra results showed interaction between N3 and NMBI could retard the aggregation of dye molecules, decreasing the electron quenching and charge recombination. However, the results of cyclic voltammograms and UV−vis absorption edge revealed the interaction between NMBI and dye molecules could cause the lowest unoccupied molecular orbital (LUMO) level of the dye molecule to drop, decreasing the electron injection efficiency. It decreased the J_{sc} of dye-sensitized solar cells (DSCs). The intercalation composite could remedy the disadvantage of NMBI and obtain strengthened interface effects. The photocurrent−voltage ($I-V$) curve showed that, with the modification of this intercalation nanocomposite, the J_{sc} of the devices increased, showing that the disadvantage caused by NMBI was improved. Besides, results of the dark current curve and transient photovoltage spectra showed the NMBI−MMT intercalation composite modification retarded charge recombination more effectively than using NMBI individually. An electrochemical impedance spectroscopy (EIS) test also indicated that modification of the NMBI−MMT intercalation composite showed a strengthened effect of retarding the charge recombination. Furthermore, the results of intensity-modulated photocurrent spectroscopy (IMPS) and intensity-modulated photovoltage spectroscopy (IMVS) tests also showed that the interface modification of the NMBI−MMT intercalation composite enhanced the electron transportation and lifetime in DSCs more than using NMBI individually.

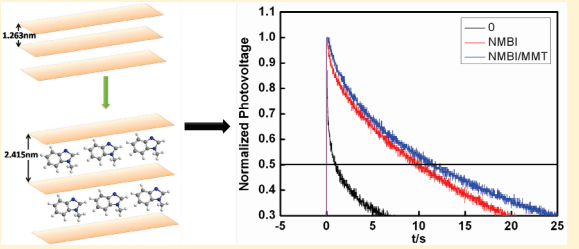

1. INTRODUCTION

As a possible low-cost alternative to inorganic photovoltaic devices, dye-sensitized solar cells (DSCs) have attracted considerable attention since 1991.[1] Conversion efficiency up to 12% has been achieved up to now.[2] However, DSCs still suffered from a range of energy losses. The conversion efficiency of DSCs could be enhanced if all the parameters are optimized.[3] Much work has been done on the dye,[4,5] photoanode,[6−9] electrolyte,[10] and counter electrode[11] to improve the performance of DSCs.

In DSCs, the charge recombination may cause a reduction of open-circuit voltage, hence decrease the conversion efficiency.[12,13] The interface of sensitized TiO_2/electrolyte is a vital factor affecting the performance of DSCs.[14] Several important reactions in DSCs occurred at this interface, such as electron injection, charge transfer, charge recombination, and dye regeneration. As a result, many studies have been done about this interface. Interface modification and additive with modification effect in electrolyte were considered as effective methods to modify the interface of sensitized TiO_2/electrolyte to improve the performance of DSCs.[15−20]

N-Methyl-benzimidazole (NMBI) is a common additive in the electrolyte of DSCs. It could retard the charge recombination between the electrons in the conductive band of TiO_2 and I^-/I_3^- in electrolyte by interacting with the TiO_2 film.[21] As a result, adding NMBI into the electrolyte weakened the back reaction, then the performance of the device was improved. However, NMBI in electrolyte slowed the transportation of I^-/I_3^- and decreased the conductivity of the electrolyte, which could decrease the conversion efficiency of DSCs. Thus, NMBI should be concentrated at the interface of sensitized TiO_2/electrolyte, remaining the advantage of retarding the charge recombination and avoiding the disadvantage of slowing the charge transportation in electrolyte.

Despite of reacting with TiO_2, NMBI could also interact with the dye molecules. With the existence of NMBI, the intermolecular hydrogen bonding of N3 dye, which caused the aggregation of dye molecules, was weakened. So the charge recombination was further retarded.

However, the interacting between NMBI and N3 dye reduces the lowest unoccupied molecular orbital (LUMO) energy level of the dye. As a result, the J_{sc} decreased with the NMBI modification. To avoid the disadvantage of NMBI and further strengthen the interface modification effects, an NMBI−MMT (montmorillonite) intercalation composite was employed. With the modification of this composite, both J_{sc} and V_{oc} were increased. Besides, the composite revealed an even stronger

Received: May 12, 2011
Revised: June 26, 2011
Published: July 14, 2011

dx.doi.org/10.1021/jp204466h | *J. Phys. Chem. C* 2011, 115, 17986–17992

effect of retarding charge recombination than using NMBI individually, which showed strengthened interface modification effects in DSCs. Furthermore, the modification of this composite enhanced the conversion efficiency of DSCs more than using NMBI individually. Thus, better modification effects were achieved by modification with the intercalation composite. Furthermore, the mechanism of interface modification effects of the NMBI−MMT intercalation composite was discussed.

2. EXPERIMENTAL SECTION

The TiO_2 colloid was prepared with a hydrothermal method, which was documented in the previous report.[22]

To prepare nanoporous TiO_2 film, transparent conductive FTO glass (12 Ω square^{-1}) was completely cleaned, and then a thin compact TiO_2 film (about 8 nm in thickness) was deposited on it to improve ohmic contact and adhesion between the porous TiO_2 layer and the FTO glass. The doctor blade technique was adopted to prepare the porous TiO_2 layer, and the thickness was controlled by an adhesive tape, which was about 10 μm thick. Afterward, the film was thermotreated at 450 °C for 30 min. After being cooled to 110 °C, the TiO_2 electrode was immersed in 0.3 mM N3 absolute ethanol solution for 12 h and cleaned with absolute ethanol.

The NMBI−MMT intercalation composite was synthesized by mixing the two materials in the 3-methoxypropionitrile (MePN) with ultrasonic vibration for 15 min, then drying in a vacuum oven at 60 °C. This intercalation composite was dispersed in a solution of 0.1 M LiI, 0.1 M I_2 in MePN, then was used to interface modification.

The composition of the quasi-solid electrolyte is as follows: 0.1 M LiI, 0.1 M I_2, 0.6 M 1,2-dimethyl-3-propyl imidazolium iodide (DMPII), 10% PEO. The solvent was MePN.[23]

A chemically platinized conductive glass was used as the counter electrode. When assembling the DSCs, the interface modification materials and polymer gel electrolyte were sandwiched in turn by a sensitized TiO_2 electrode and a counter electrode with two clips. Finally, the DSCs were baked at 80 °C for 20 min.

Photocurrent−voltage (I−V) and dark current measurements were performed by a Keithley model 4200-SCS semiconductor characterization system with real-time plotting and analysis with an active area of 0.25 cm^2. X-ray diffraction (XRD) results were obtained with an X-ray powder diffractometer (D/max2550HB+/PC). The transient photovoltages of the DSCs were studied by probing the cells with a weak laser pulse at 532 nm, which was generated by a frequency-doubled Nd:YAG laser. The transient photovoltage signal was tested under the open-circuit condition and recorded utilizing a TDS220 oscilloscope (Tektronix). Electrochemical impedance spectroscopy (EIS), cyclic voltammograms, intensity-modulated photovoltage spectroscopy (IMVS), and intensity-modulated photocurrent spectroscopy (IMPS) were tested by a Zanner CIMPS electrochemical workstation, Germany. And the frequency of the EIS ranged from 0.1 to 10^5 Hz. The cyclic voltammograms test was carried out in a conventional photoelectrochemical cell equipped with a 2 mm gold electrode as the working electrode, a platinum disk electrode as the counter electrode, and a Ag/AgCl reference electrode in pure DMF solvent. The solution concentration was 2×10^{-3} M, with 0.1 M TBATFB electrolyte.

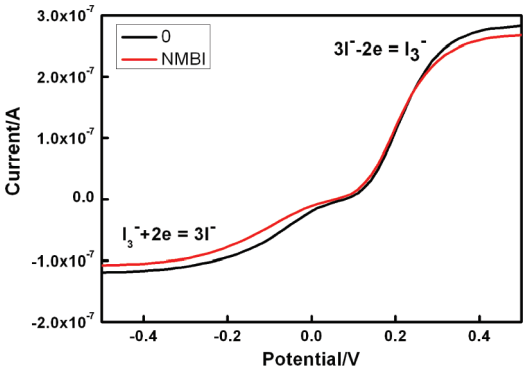

Figure 1. Steady-state voltammograms of electrolytes with and without NMBI.

Table 1. Steady-State Currents, Diffusion Coefficients of I^-/I_3^-, and Conductivities of Electrolytes with and without NMBI

samples	$10^7 I_{ss}$ $(I_3^-)/A$	$10^{10} D_{app}$ $(I_3^-)/m^2\ s^{-1}$	$10^7 I_{ss}$ $(I^-)/A$	$10^{10} D_{app}$ $(I^-)/m^2\ s^{-1}$	σ/mS/cm
0	2.821	3.664	1.190	0.774	6.45
NMBI	2.671	3.469	1.074	0.699	4.67

3. RESULTS AND DISCUSSION

3.1. Interface Modification Effects of NMBI. The charge transport properties of the I^-/I_3^- redox couple in electrolyte were important for the performance of DSCs. Generally, the faster the I^-/I_3^- redox couple transport, the higher the conversion efficiency of the DSCs was. The steady-state voltammetry could be used to measure the apparent diffusion coefficient of the I^-/I_3^- redox couple. The apparent diffusion coefficient (D_{app}) values of I^-/I_3^- were calculated from the anodic and cathodic steady-state current (I_{ss}) using the following equation:[24]

$$I_{ss} = 4naCFD_{app} \quad (1)$$

where n is the electron number in the electrode reaction, a is the radius of the Pt ultramicroelectrode, C is the bulk concentration of electroactive species, F is the Faraday constant, and D_{app} is the apparent diffusion coefficient.

Figure 1 shows the steady-state voltammograms of the quasi-solid electrolyte with and without NMBI added. As shown in Figure 1 and Table 1, the diffusion coefficient (D_{app}) values of I^-/I_3^- decreased with NMBI added. It showed that the NMBI in the electrolyte slowed the transportation of I^-/I_3^-. Furthermore, as shown in Table 1, adding NMBI into the electrolyte decreased the conductivity. Thus, to avoid this disadvantage, NMBI should be concentrated at the interface of sensitized TiO_2/electrolyte rather than adding it into the electrolyte.

The oversaturation adsorption of N3 dye suffers from the problem of dye aggregation, which could increase the interface resistance, then decrease the efficiency of DSCs.[25] Wenger et al. reported that the aggregated state of the dye slowed electron injection in DSCs, which may lead to the reductive quenching of N3 derivatives.[26] The results of X-ray analysis of an N3 single crystal showed the interaction between the dye molecules was hydrogen bonding.[26] The structural models also demonstrated that there were two or three free carboxylic groups, which did not come in contact with the surface when the N3 dye molecules

were absorbed onto TiO_2 films.[26] These free carboxylic groups may cause the hydrogen-bonding aggregation, hence lowering the performance of the DSCs.

Because of the alkalinity of NMBI, besides of the interaction with TiO_2, it could interact with the dye molecules. To explore the interaction between NMBI and dye, FTIR spectra for photoanodes of TiO_2/N3 and TiO_2/N3/NMBI were tested.

As shown in Figure 2, the 2114 cm^{-1} peak assigned to the −SCN group was observed in both samples without change, as the −SCN group could only come from the dye molecule, and the group number was consistent with the molecule number. The peak of the 3000−3400 cm^{-1} range was attributed to the stretching vibrations of the −O−H in the −COOH group. It was wide due to the existing of intermolecular hydrogen bonding. As shown in Figure 2, with NMBI coating, the peak was weakened, showing the intermolecular hydrogen bonding of dye molecules causing aggregation was weakened. Thus, it could be judged that NMBI could retard the aggregation of dye molecules. Furthermore, with NMBI coating, the intensity of the 1720 cm^{-1} peak assigned to the −C═O group in COOH decreased obviously, further showing the interaction between −COOH of N3 and NMBI retarded the formation of intermolecular hydrogen bonding. Thus, the aggregation of N3 dye was weakened by NMBI, which could decrease the charge recombination in DSCs.

As shown in Figure 2, with NMBI modification, the reductive quenching of N3 caused by the aggregation was retarded, which could improve the performance of DSCs. It was known that the optical band gap (E_g) for direct interband transitions and the absorption coefficient (A) near the absorption edge have a relationship that complied with the following formula[27]

$$(Ahv)^2 = c(hv - E_g) \quad (2)$$

where the optical band gap for the absorption edge can be obtained by extrapolating the linear portion of the plot $(Ahv)^2$−hv to $A = 0$.[28] As shown in Figure 3a, the optical band gap of N3 dye was red-shifted with the coating of NMBI, which suggested that the E_g of N3 became smaller when NMBI was added.

Besides making the conduction band shift upward, interaction between NMBI and N3 also changed the energy level of dye molecules. To explore the energy level change of N3 with NMBI modification, cyclic voltammograms (CV) of the N3 dye and N3/NMBI in pure DMF solvent were tested. As shown in Figure 3b, the reduction potential of N3 and N3/NMBI was −1.10 and −0.93 V, which became more positive. The result of the CV test showed that, with the adding of NMBI, the LUMO level of the N3 dye dropped, which is shown in Figure 4. The LUMO of N3 was higher than the energy level of the conductive band of TiO_2, which was why the electron could be injected from the dye molecule into the TiO_2 film.[29] When the LUMO level dropped, the driven force of electron injection decreased, which could cause the J_{sc} decrease, being a negative effect for the performance of DSCs.

3.2. Interface Modification Effects of the NMBI−MMT Intercalation Composite. As discussed above, NMBI could decrease charge recombination effectively by weakening the aggregation of dye molecules. However, it made the LUMO of N3 dye drop, which could cause the J_{sc} decrease. To weaken the

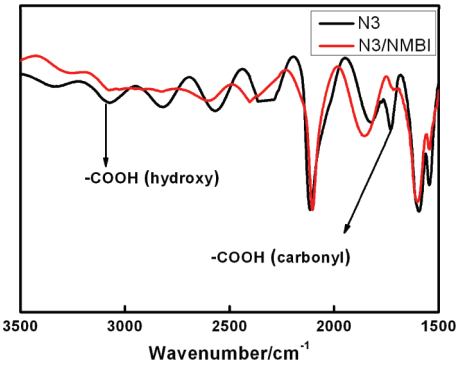

Figure 2. FTIR spectra for photoanodes of TiO_2/N3 and TiO_2/N3/NMBI.

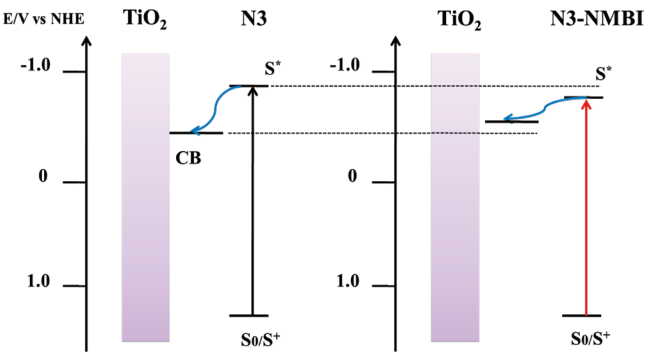

Figure 4. Energy levels of the TiO_2 and the N3 dye without and with NMBI.

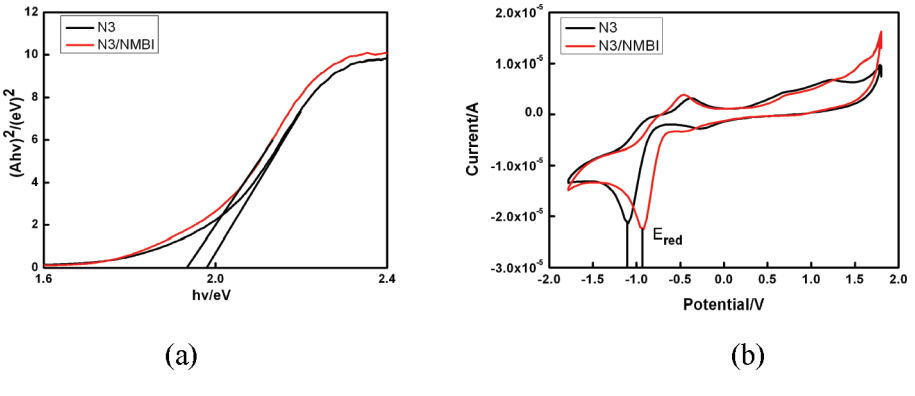

Figure 3. (a) $(Ahv)^2$ vs hv curves of the N3 dye with and without modification of NMBI. (b) Cyclic voltammograms of N3 and N3/NMBI in DMF.

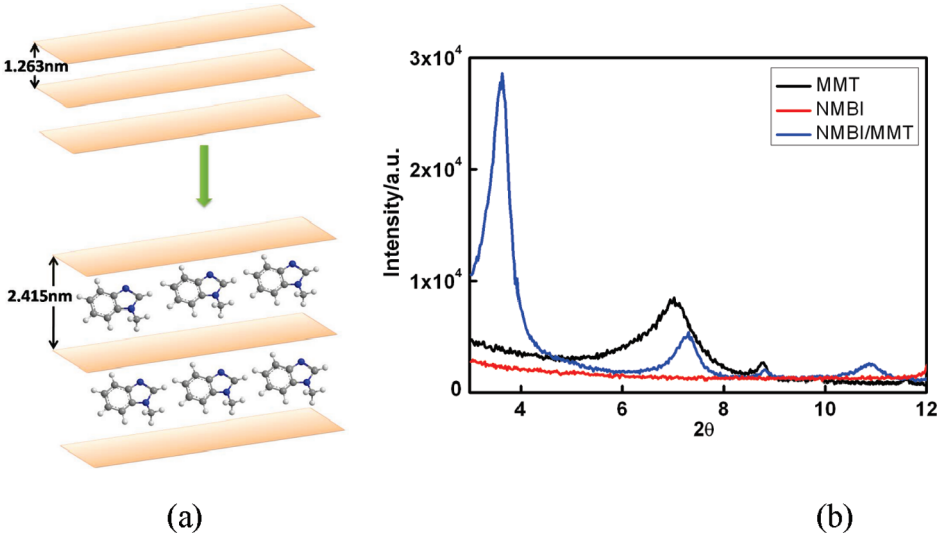

Figure 5. (a) Diagrammatic sketch and (b) X-ray diffraction spectra of MMT, NMBI, and NMBI−MMT.

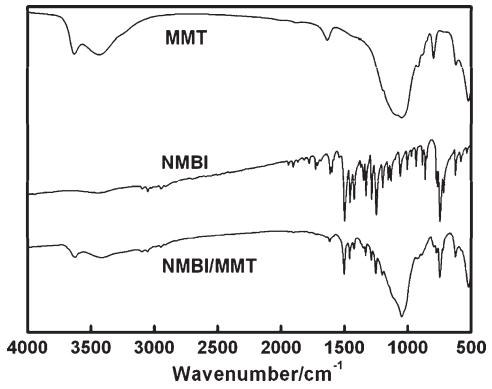

Figure 6. FTIR spectra of NMBI, MMT, and NMBI−MMT intercalation composite.

Table 2. Performance of DSCs without and with Interface Buffer Structure Containing Different Materials

sample	V_{oc}/V	J_{sc}/mA/cm^2	FF%	η%
0	0.61	11.12	51.9	3.52
NMBI	0.68	10.96	64.1	4.78
NMBI−MMT	0.72	11.90	65.2	5.59

disadvantages of NMBI that decreased J_{sc} and obtain a better modification effect, a novel intercalation nanocomposite of MMT and NMBI was synthesized and applied to interface modification in DSCs.

Figure 5a shows the structure of NMBI−MMT nanocomposite. NMBI intercalated into the interlayer spacing of MMT. To confirm the intercalation structure, the X-ray diffraction spectra of MMT, NMBI, and NMBI−MMT intercalation composite were tested. As shown in Figure 5b, the peak at $2\theta = 7°$ corresponds to the basal interlayer spacing of MMT. And pure NMBI had no peak when the reflection angle 2θ was smaller than 12°. After the intercalation, the peak greatly shifted to smaller reflection angles due to expansion produced by intercalated NMBI. The interlayer spacing (d) and the interlayer expansion (Δd) compared to pure MMT calculated from the powder X-ray diffraction data were summarized. The interlayer spacing of MMT (d) is 1.263 nm, which increased to 2.415 nm due to the intercalation of NMBI. The value of interlayer expansion (Δd) was 1.152 nm.

The intercalation rates (IR) given as percentage were calculated from the X-ray diffraction spectra data, as described in the follow equation:[30]

$$IR\% = I_i \times 100\%/(I_i + I_k) \quad (3)$$

where I_i was the peak intensity observed for intercalated MMT and I_k was the peak intensity observed for pure MMT. The results showed that the intercalation rate of NMBI in the composite was 84.4%. Accordingly, intercalation of NMBI into MMT was confirmed.

Figure 6 showed the FTIR spectra of NMBI, MMT, and the NMBI-MMT intercalation composite. As shown in the Figure 6, The presence of MMT in the nanocomposites can be evidenced by its absorption pattern in the 3300−3600 cm^{-1} range.[31] The two bands observed in this region of spectrum (3627, 3418 cm^{-1}) can be assigned to the OH stretching of MMT. Compared to the pure MMT, the intensity of the two peaks decreased sharply, and the peak of 3418 cm^{-1} nearly disappeared, which indicated that the interactivity of NMBI and MMT in the composite weakened the −OH of MMT. The presence of NMBI can be evidenced by absorption peaks around 1595, 1539, and 1513 cm^{-1} that were due to phenyl stretching vibrations. The absorption peak around 1050 cm^{-1} was from stretching vibration of Si−O−Si. Compared to the pure MMT, the peak of 1050 cm^{-1} of NMBI−MMT composite changed much sharper, which indicated that the interaction between NMBI and MMT in the composite affected the Si−O−Si.

The NMBI−MMT intercalation composite was used in interface modification of DSCs. As shown in Table 2 and Figure 7a, compared to the blank sample, the device with NMBI modification obviously enhanced the V_{oc} and fill factor (FF), which increased from 0.61 to 0.68 V and 51.9% to 64.1%, respectively. However, the J_{sc} decreased due to the raising of flat-band

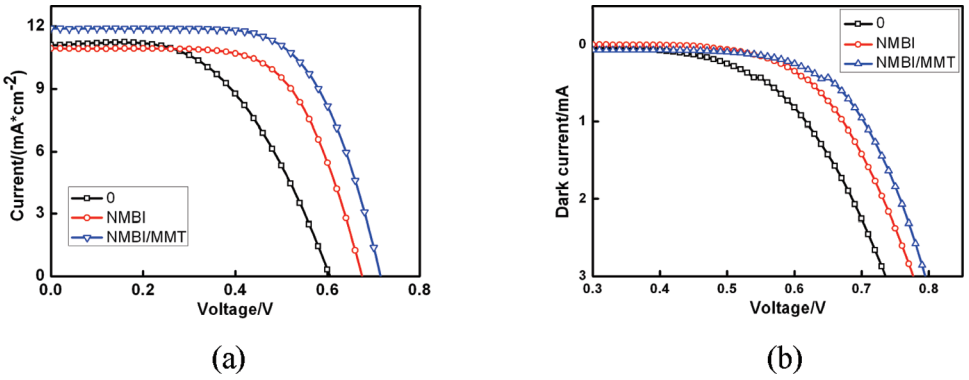

Figure 7. (a) $I-V$ curves and (b) dark current curves of cells without and with interface modifications of different materials.

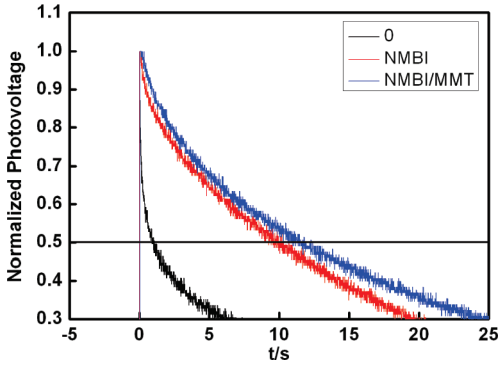

Figure 8. Normalized transient photovoltage spectra for cells without and with an interface buffer structure containing different materials.

potential and dropping of the LUMO energy level of N3, which was shown in Figure 4. Meantime, with modification of the intercalation composite, the V_{oc} of the device with the composite modification not only was higher than that of the blank sample, but also higher than that with NMBI modification individually, which increased further from 0.68 to 0.72 V. The J_{sc} also became higher, which increased from 10.96 to 11.90 mA/cm^2. As a result, the NMBI−MMT composite modification enhanced both V_{oc} and J_{sc} of DSCs. It strengthened the effects of NMBI on V_{oc} and fill factor, indicating that the MMT in the composite was synergetic for the interface modification effects. Compared to the blank sample, the conversion efficiency of the device with NMBI−MMT composite increased significantly from 3.52% to 5.59% using quasi-solid electrolyte, which was also more than that with NMBI individually.

As shown in Figure 7b, the dark current of the device with NMBI decreased obviously. However, the dark current of the device with NMBI−MMT composite modification further reduced to a lower level compared to individual NMBI modification. It indicated that, while the NMBI−MMT intercalation composite was employed, a further decreasing of charge recombination in DSCs than using NMBI only was achieved.

To further discuss the charge recombination in different devices, the transient photovoltages measurements carried out under the open-circuit condition denoted the decay rate of the injected electrons. The slower the decay was, the weaker the charge recombination process was. As shown in Figure 8, the decay rate of injected electron was in the order of NMBI−MMT composite < NMBI < blank sample. Thus, the order of charge recombination was opposite. This result revealed that the NMBI−MMT composite slowed down the decaying of injected electrons with a maximum extent, showing a best effect of retarding the charge recombination. It was also consistent with the results of the dark current curves. It further confirmed that, compared with using NMBI individually, the interface modification effect was strengthened when the composite was applied.

As DSC can be considered as a leaking capacitor in dark condition,[32] the resistance of the back-reaction from TiO_2 to the triiodide ions in the electrolyte was analyzed through the EIS technique under dark condition. The resistance at the interface of the sensitized TiO_2/electrolyte was presented by the semicircle in intermediate frequency range of the Nyquist plots.[33] When the diameter of the middle frequency semicircle was bigger, the electron recombination at the sensitized TiO_2/electrolyte interface was slighter.[34]

Figure 9a shows the Nyquist plots of DSCs with different modification materials measured at −0.8 V bias voltage in dark condition and the equivalent circuits. The R_2 in the equivalent circuit represented the interfacial resistance of sensitized TiO_2/electrolyte. The radii of the intermediate frequency semicircles, which revealed the R_2 in the equivalent circuit, were in the order of NMBI−MMT composite > NMBI > blank sample. The Nyquist plot revealed the electron recombination at the sensitized TiO_2/electrolyte interface decreased in order when it was modified by NMBI individually and by NMBI−MMT composite. It also accorded with the trends in the values of V_{oc}. As a result, the modification of NMBI−MMT composite achieved a better effect of retarding the charge recombination in DSCs than using NMBI individually, which was corresponding with the values of V_{oc} and the results of dark current measurement.

Under an illumination condition, the DSCs could be taken as diodes.[27] The resistance at the sensitized TiO_2/electrolyte interface was also presented by the middle frequency semicircle in the Nyquist plots. The equivalent circuit under illumination condition was also the same as shown in Figure 9a. As shown in Figure 9b, the results of the illumination EIS test revealed that the interface modification of NMBI−MMT composite did not slow the electron transfer and collection at the sensitized TiO_2/electrolyte interface. And it was evidenced by the intermediate frequency semicircle radius of the device with modification of the composite that did not increase but decreased slightly.

The results of EIS showed that the interface modification with the intercalation composite retarded the charge recombination

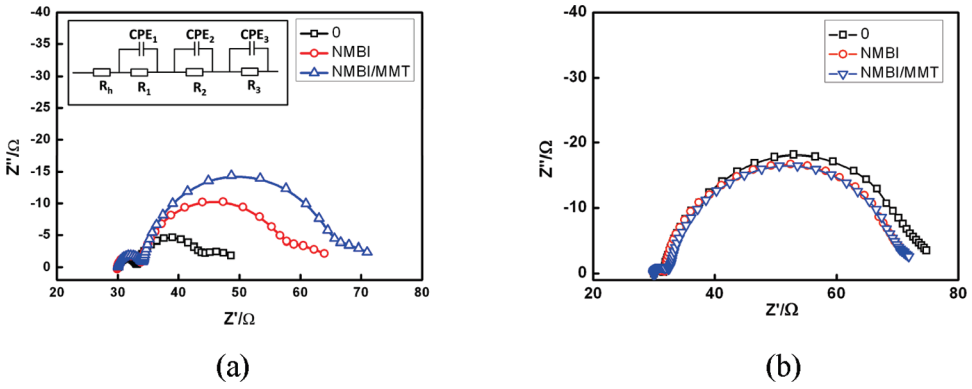

Figure 9. Nyquist plots of DSCs without and with different modification materials (a) in dark and (b) under illumination condition.

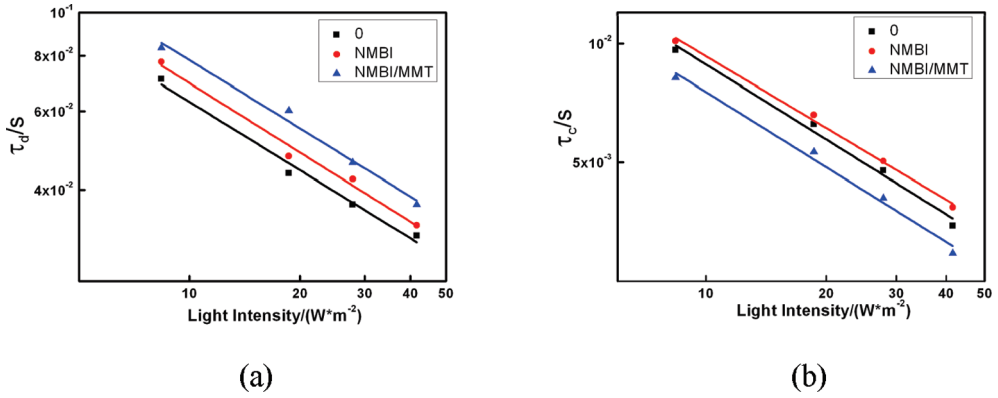

Figure 10. (a) IMVS and (b) IMPS spectra of devices with different modification materials.

but had no adverse impact on electron transfer at the sensitized TiO_2/electrolyte interface.

To explore the influence of the interface modification on the electron diffusion and lifetime in DSCs, IMVS and IMPS spectra of devices based on different modification materials were tested. The IMVS experiment used the same intensity perturbation but measured the periodic modulation of the photovoltage, giving the information of electron lifetime under open-circuit conditions.[35] As shown in Figure 10a, with NMBI modification, the electron lifetime increased, while it increased furthermore when the NMBI−MMT intercalation composite was used. It indicated that the intercalation composite had a strengthened effect of enhancing electron lifetime than that of NMBI individually. It was due to the stronger effect of retarding charge recombination. The results were also accorded with the value of V_{oc} and results of the EIS test. IMPS measured the periodic photocurrent response of the device to a small sinusoidal perturbation of the light intensity superimposed on a larger steady background level, providing information about the dynamics of charge transport and back-reaction under short-circuit conditions.[36] As shown in Figure 10b, with NMBI modification, the electron collection time increased a little, which meant the electron diffusion in TiO_2 film was slowed. It indicated that NMBI was detrimental for the electron diffusion, which was also shown in the steady-state voltammograms and conductivity test, though this effect was slighter than when it was located at the interface of the photoanode/electrolyte than it was added in the electrolyte. The effect of NMBI weakening dye aggregation and retarding charge recombination was beneficial to the electron injection. However, it dropped the LUMO energy level and shifted the conductivity band of TiO_2 up, decreasing the injection driven force and charge transfer at the interface of sensitized dye/electrolyte meanwhile. When using NMBI individually, the latter was more obvious. Thus, the collection time increased, showing lower electron diffusion. When NMBI−MMT intercalation composite was applied, the collection time decreased to a lower level than that of the blank sample, meaning the electron diffusion was improved. It also accorded with the value of J_{sc}. It could be explained that using the intercalation composite, diffusion of NMBI to the electrolyte was decreased. Besides, MMT was also beneficial to the electron transportation in DSCs.[37] Furthermore, forming the intercalation composite, due to the steric hindrance of MMT, it retarded the dye aggregation and charge recombination more effectively. Then the beneficial effect became more important. As a result, this intercalation composite made up the defect of NMBI that slowed the electron diffusion, and strengthened the interface modification effects meanwhile. This was why it could enhance the conversion efficiency of devices more than that using NMBI individually.

The mechanism of strengthened effects of intercalation composite was also discussed. This strengthened modification effect was caused by the introducing of MMT in the intercalation composite. NMBI adsorbed on the surface of sensitized TiO_2 film, then pulled MMT in the composite to concentrate at the interface of sensitized TiO_2/electrolyte by the interaction between NMBI and the photoanode. As an insulator, MMT in the intercalation could further retard the charge recombination.

dx.doi.org/10.1021/jp204466h |J. Phys. Chem. C 2011, 115, 17986–17992

Furthermore, the intercalation composite prevented NMBI at the interface of sensitized TiO_2/electrolyte diffusion to the electrolyte bulk, which could weaken the modification effect of NMBI. Thus, the modification effect of NMBI was further strengthened, which was evidenced by the results of dark current measurement and transient photovoltage measurement. Besides, the retarding of NMBI diffusion weakened its blocking effect of electron transportation in electrolyte, which was beneficial to enhance the J_{sc}.

4. CONCLUSION

In summary, first, interaction of NMBI with N3 dye molecules was studied. The FTIR spectra results showed the aggregation of dye molecules was retarded with NMBI modification, decreasing the electron quenching and charge recombination. However, the results of cyclic voltammograms and UV−vis absorption edge revealed the interaction between NMBI and dye molecules could cause the energy level of the dye molecule to drop, decreasing the electron injection efficiency of DSCs. Thus, the J_{sc} decreased. To complement the disadvantage of NMBI and obtain a better interface modification effect, an NMBI−MMT intercalation nanocomposite was first applied for interface modification. The XRD results showed the interlayer spacing of MMT became larger with NMBI intercalated, confirming the formation of an intercalation nanocomposite. The results of the $I-V$ curve showed that modification of this composite increased the J_{sc}, with a better effect than that of individual NMBI, which could decrease the J_{sc}. Furthermore, the intercalation composite modification could enhance V_{oc} and FF with a more greater degree than that with individual NMBI modification. Compared to the blank sample, the conversion efficiency increased from 3.52% to 5.59% using quasi-solid electrolyte. Besides, the results of transient photovoltage spectra and the dark current curve showed that the charge recombination process was significantly retarded, which showed strengthen modification effects compared to traditional modification with only one material.

AUTHOR INFORMATION

Corresponding Author

*E-mail: chldwang@mail.tsinghua.edu.cn. Phone: (008610) 627-88802. Fax: (008610) 62795137.

ACKNOWLEDGMENT

This work was supported by the National Natural Science Foundation of China under Grant No. 50873055 and the National Key Basic Research and Development Program of China under Grant No. 2009CB930602.

REFERENCES

(1) O'Regan, B.; Grätzel, M. *Nature* **1991**, *353*, 737.
(2) (a) Grätzel, M. *Acc. Chem. Res.* **2009**, *42*, 1788.(b) Grätzel, M. Presented at the 4th International Conference on the Industrialisation of Dye Solar Cells, Colorado Springs, CO, 2010.
(3) Frank, A. J.; Kopidakis, N.; van de Lagemaat, J. *Coord. Chem. Rev.* **2004**, *248*, 1165.
(4) Tian, H. N.; Yang, X. C.; Chen, R. K.; Hagfeldt, A.; Sun, L. C. *Energy Environ. Sci.* **2009**, *2*, 674.
(5) Burke, A.; Schmidt-Mende, L.; Ito, S.; Grätzel, M. *Chem. Commun.* **2007**, 234.
(6) Enache-Pommer, E.; Liu, B.; Aydil, E. S. *Phys. Chem. Chem. Phys.* **2009**, *11*, 9648.
(7) Yu, Q. J.; Zhou, D. F.; Shi, Y. H.; Si, X. Y.; Wang, Y. H.; Wang, P. *Energy Environ. Sci.* **2010**, *3*, 1722.
(8) Joshi, P.; Zhang, L. F.; Davoux, D.; Zhu, Z. T.; Galipeau, D.; Fong, H.; Qiao, Q. Q. *Energy Environ. Sci.* **2010**, *3*, 1507.
(9) Gajjela, S. R.; Ananthanarayanan, K.; Yap, C.; Grätzel, M.; Balaya, P. *Energy Environ. Sci.* **2010**, *3*, 838.
(10) Lan, Z.; Wu, J. H.; Hao, S.; Lin, J. M.; Huang, M. L.; Huang, Y. F. *Energy Environ. Sci.* **2009**, *2*, 524.
(11) Lee, K. M.; Hsu, C. Y.; Chen, P. Y.; Ikegami, M.; Miyasaka, T.; Ho, K. C. *Phys. Chem. Chem. Phys.* **2009**, *11*, 3375.
(12) Diamant, Y.; Chen, S. G.; Melamed, O.; Zaban, A. *J. Phys. Chem. B* **2003**, *107*, 1977.
(13) Bandaranayake, K. M. P.; Senevirathna, M. K. I.; Weligamuwa, P.; Tennakone, K. *Coord. Chem. Rev.* **2004**, *248*, 1277.
(14) Fang, J. H.; Mao, H. F.; Wu, J. W.; Zhang, X. Y.; Lu, Z. H. *Appl. Surf. Sci.* **1997**, *119*, 237.
(15) Liu, Z. Y.; Pan, K.; Liu, M.; Wang, M. J.; Lu, Q.; Li, J. H.; Bai, Y. B.; Li, T. J. *Electrochim. Acta* **2005**, *50*, 2583.
(16) Chen, S. G.; Chappel, S.; Diamant, Y.; Zaban, A. *Chem. Mater.* **2001**, *13*, 4629.
(17) Palomares, E.; Clifford, J. N.; Haque, S. A.; Lutz, T.; Durrant, J. R. *J. Am. Chem. Soc.* **2003**, *125*, 475.
(18) Gao, R.; Wang, L. D.; Ma, B. B.; Zhan, C.; Qiu, Y. *Langmuir* **2010**, *26*, 2460.
(19) Luo, F.; Wang, L. D.; Ma, B. B.; Qiu, Y. *J. Photochem. Photobiol., A* **2008**, *197*, 375.
(20) Fischer, A.; Pettersson, H.; Hagfeldt, A.; Boschloo, G.; Kloo, L.; Gorlov, M. *Sol. Energy Mater. Sol. Cells* **2007**, *91*, 1062.
(21) Zhang, C. N.; Dai, J.; Huo, Z. P.; Pan, X.; Hu, L. H.; Kong, F. T.; Huang, Y.; Sui, Y. F.; Fang, X. Q.; Wang, K. J.; Dai, S. Y. *Electrochim. Acta* **2008**, *53*, 5503.
(22) Burnside, S. D.; Shklover, V.; Barbé, C.; Comte, P.; Arendse, F.; Brooks, K.; Grätzel, M. *Chem. Mater.* **1998**, *10*, 2419.
(23) Shi, Y. T.; Zhan, C.; Wang, L. D.; Ma, B. B.; Gao, R.; Zhu, Y. F.; Qiu, Y. *Phys. Chem. Chem. Phys.* **2009**, *11*, 4230.
(24) Quinn, B. M.; Ding, Z. F.; Moulton, R.; Bard, A. J. *Langmuir* **2002**, *18*, 1734.
(25) Koide, N.; Islam, A.; Chiba, Y.; Han, L. Y. *J. Photochem. Photobiol., A* **2006**, *182*, 296.
(26) Wenger, B.; Grätzel, M.; Moser, J. E. *J. Am. Chem. Soc.* **2005**, *127*, 12150.
(27) Kilsa, K.; Mayo, E. I.; Brunschwig, B. S.; Gray, H. B.; Lewis, N. S.; Winkler, J. R. *J. Phys. Chem. B* **2004**, *108*, 15640.
(28) Tsunekawa, S.; Fukuda, T.; Kasuya, A. *J. Appl. Phys.* **2000**, *87*, 1318.
(29) Zeng, J.; Xin, M. D.; Li, K. W.; Wang, H.; Yan, H.; Zhang, W. J. *J. Phys. Chem. C* **2008**, *112*, 4159.
(30) Uwins, P. J. R.; Mackinnon, I. D. R.; Thompson, J. G.; Yago, A. J. E. *Clays Clay Miner.* **1993**, *41*, 707.
(31) Qiao, M.; Wu, S. S.; Ran, Q. P.; Shen, J. *Polym. Adv. Technol.* **2010**, *21*, 296.
(32) Bisquert, J. *J. Phys. Chem. B* **2002**, *106*, 325.
(33) Wang, Q.; Moser, J.; Grätzel, M. *J. Phys. Chem. B* **2005**, *109*, 14945.
(34) Huo, Z. P.; Dai, S. Y.; Wang, K. J.; Kong, F. T.; Zhang, C. N.; Pan, X.; Fang, X. Q. *Sol. Energy Mater. Sol. Cells* **2007**, *91*, 1959.
(35) Schlichthörl, G.; Huang, S. Y.; Sprague, J.; Frank, A. J. *J. Phys. Chem. B* **1997**, *101*, 8141.
(36) Dloczik, L.; Ileperuma, O.; Lauermann, I.; Peter, L. M.; Ponomarev, E. A.; Redmond, G.; Shaw, N. J.; Uhlendorf, I. *J. Phys. Chem. B* **1997**, *101*, 10281.
(37) Ito, B. I.; de Freitas, J. N.; Paoli, M.-A. D.; Nogueira, A. F. *J. Braz. Chem. Soc.* **2008**, *19*, 688.